Protein Stabilization by Introduction of Cross-Strand Disulfides†

Kausik Chakraborty,‡ Sudhir Thakurela,‡ Ravindra Singh Prajapati,‡ S. Indu,‡ P. Shaik Syed Ali,‡ C. Ramakrishnan,‡ and Raghavan Varadarajan*,‡,⊥

Molecular Biophysics Unit, Indian Institute of Science, Bangalore 560 012, India, and Chemical Biology Unit, Jawaharlal Center for Advanced Scientific Research, Jakkur P.O., Bangalore 560 004, India

Received May 18, 2005; Revised Manuscript Received September 10, 2005

ABSTRACT: Disulfides cross-link residues in a protein that are separated in primary sequence and stabilize the protein through entropic destabilization of the unfolded state. While the removal of naturally occurring disulfides leads to protein destabilization, introduction of engineered disulfides does not always lead to significant stabilization of a protein. We have analyzed naturally occurring disulfides that span adjacent antiparallel strands of β sheets (cross-strand disulfides). Cross-strand disulfides have recently been implicated as redox-based conformational switches in proteins such as gp120 and CD4. The propensity of these disulfides to act as conformational switches was postulated on the basis of the hypothesis that this class of disulfide is conformationally strained. In the present analysis, there was no evidence to suggest that cross-strand disulfides are more strained compared to other disulfides as assessed by their torsional energy. It was also observed that these disulfides occur solely at non-hydrogen-bonded (NHB) registered pairs of adjacent antiparallel strands and not at hydrogen-bonded (HB) positions as suggested previously. One of the half-cystines involved in cross-strand disulfide formation often occurs at an edge strand. Experimental confirmation of the stabilizing effects of such disulfides was carried out in *Escherichia coli* thioredoxin. Four pairs of cross-strand cysteines were introduced, two at HB and two at NHB pairs. Disulfides were formed in all four cases. However, as predicted from our analysis, disulfides at NHB positions resulted in an increase in melting temperature of 7−10 °C, while at HB positions there was a corresponding decrease of −7 °C. The reduced state of all proteins had similar stability.

Disulfides cross-link residues that are widely spaced in the primary sequence of a protein and have an important role to play in the stability, structural integrity, and folding of proteins. The mechanism of protein stabilization by disulfides is generally attributed to the entropic destabilization of the unfolded state of a protein with respect to its native state (*1*, *2*). Engineering de novo disulfides to increase protein stability has been attempted with varying degrees of success (*3*−*7*). While the removal of naturally occurring disulfides leads to protein destabilization, introduction of an engineered disulfide does not always lead to significant stabilization of a protein (*8*, *9*). This is possibly because the engineered disulfides cannot be sterically accommodated without rearrangement of surrounding residues. Such rearrangements have an energetic cost.

Disulfides within a β sheet have been recently implicated as redox-based conformational switches (*10*, *11*). Characterization of disulfide stereochemistry in general and cross-strand disulfides in particular has been carried out previously (*12*). That characterization was based on only 20 disulfides from high-resolution structures (resolution better than 2.0 Å) and an additional 50 from lower resolution structures, and hence the results needed to be reevaluated with a much larger dataset that is presently available.

In this study, we have carried out a comprehensive analysis of the stereochemistry of cross-strand disulfides present between two adjacent antiparallel strands of a β sheet in the Protein Data Bank (PDB). These cross-strand disulfides were compared with the other disulfides present in the dataset to look for any features that might suggest that the cross-strand disulfides are less stable than other disulfides. We found no evidence that the cross-strand disulfides are strained. We have also experimentally verified predictions from our database analysis by introducing interstrand disulfides at four pairs of positions in *Escherichia coli* thioredoxin (Trx). We demonstrate that introduction of interstrand disulfides between non-hydrogen-bonded (NHB)[1] residue pairs can result in significant protein stabilization.

MATERIALS AND METHODS

Database and Structural Analysis. A set of nonredundant, high-resolution (better than 2.5 Å) crystal structures obtained from the PISCES database (*13*) were chosen for analysis. The dataset consisted of 2887 polypeptide chains containing

† This work was supported by grants from Council of Scientific and Industrial Research and Department of Science and Technology, Government of India. R.V. is a recipient of a Swarnajayanthi Fellowship (Government of India) and is a Senior Research Fellow of the Wellcome Trust.

* Corresponding author. E-mail: varadar@mbu.iisc.ernet.in. Phone: 91-80-22932612. Fax: 91-80-23600535.

‡ Indian Institute of Science.

⊥ Jawaharlal Center for Advanced Scientific Research.

[1] Abbreviations: HB, hydrogen-bonded; NHB, non-hydrogen-bonded; GdmCl, guanidinium chloride; DSC, differential scanning calorimetry; DTNB, 5,5′-dithiobis-(2-nitrobenzoic acid); Wt*, D2PA108P *E. coli* thioredoxin; CGH10, citrate 10 mM, glycine 10 mM, HEPES 10 mM.

10.1021/bi050921s CCC: $30.25
Published on Web 10/14/2005

Table 1: Properties of Positions Chosen to Introduce Cross-Strand Disulfides in *E. coli* Thioredoxin

				side chain accessibility (%)	
construct name	N terminal residue	C terminal residue	registered pair type	N-terminal residue	C-terminal residue
77c	77T	91V	NHB	1	56
78c	78L	90K	HB	0	39
79c	79L	89T	NHB	0	25
80c	80L	88A	HB	0	28

1422 disulfides. An in house software was developed that classified the location of all half cystine residues with respect to their secondary structural attributes. The program uses the information provided in the "HELIX", "SHEET", and "SSBONDS" records of the PDB file to obtain all disulfides present between adjacent antiparallel strands of a β sheet. Such cysteine residues were also classified as being in either hydrogen-bonded pairs or non-hydrogen-bonded pairs using an in house program and were cross-checked by visual inspection. The PDB structures were visualized in Rasmol (*14*).

Definition of Geometrical Parameters. There are two types of residue pairs found in the registry between antiparallel adjacent β strands, hydrogen-bonded and non-hydrogen-bonded (*15*). In a hydrogen-bonded pair (HB), the residues are hydrogen bonded to each other by their amide hydrogen and carbonyl oxygen, whereas in a non-hydrogen-bonded pair (NHB), the residues have their amide hydrogen and carbonyl oxygen atoms facing away from each other. Side chain dihedral angles were defined using standard notation as defined earlier (*12*, *16*). The strain related to side chain torsion angles for each disulfide was calculated using the AMBER force field parameters (*17*) from the equation

$$E\ (\text{kcal/mol}) = 2(1 + \cos(3\chi_1)) + 2(1 + \cos(3\chi_{1'})) + (1 + \cos(3\chi_2)) + (1 + \cos(3\chi_{2'})) + 3.5(1 + \cos(2\chi_3)) + 0.6(1 + \cos(3\chi_3)) \quad (1)$$

where E is the strain energy in kcal/mol and χ_1, χ_2, χ_3, $\chi_{2'}$, and $\chi_{1'}$ are the standard side chain torsion angles of disulfide bonds.

Design of Thioredoxin Mutants. All mutants were designed on the basis of the crystal structure of oxidized *E. coli* thioredoxin (Trx) (PDB code 2TRX) (*18*) obtained from the Protein Data Bank (PDB). To generate mutants that bridge either NHB pairs or HB pairs of adjacent strands, we chose one residue of each pair from an edge strand of the β sheet in Trx. This was done because we observed that naturally occurring cross-strand disulfides are predominantly found between an edge strand and an adjacent antiparallel strand of a β sheet. The double mutants constructed were 77C and 91C, 78C and 90C, 79C and 89C, and 80C and 88C hereafter referred to as 77c, 78c, 79c, and 80c, respectively. The percentage side chain accessibilities of the residues and the hydrogen bonding nature of each pair are summarized in Table 1.

Constructs, Mutagenesis, Expression and Purification of Trx and Its Mutants. Trx containing the mutations D2P and A108P has slightly higher expression levels and stability (average ΔT_m of 3.1 °C in the pH range 6−10) than the wild-type Trx (Prajapati and Varadarajan, unpublished results) and was hence used as the background construct to introduce additional disulfides. Neither of these residues is close to any site being mutated. The above protein is hereafter referred to as Wt*. Wt* was cloned into pET20b (Novagen) with ampicillin as the selection marker. Wt* was mutated using the mega-primer method (*19*) to generate the various double cysteine mutants. The whole gene for each construct was sequenced to confirm the mutation. The proteins were expressed in *E. coli* strain BL21(DE3). Briefly, the cells were grown to saturation and pelleted by centrifugation. The pellet from 1 L of culture was resuspended in 10 mL of Luria broth. An equal volume of chloroform was added to the suspension. Following chloroform shock (*20*) (incubation at room temperature for 20 min with intermittent shaking), 100 mL of buffer (20 mM tris, 25 mM NaCl, pH 7.4) was added. Centrifugation at 4000 rpm at 4 °C was done to separate the chloroform layer from aqueous layer. The aqueous layer was loaded onto a Q-sepharose column equilibrated with 20 mM tris (pH 7.4). The column was washed with 20 mM tris, 25 mM NaCl (pH 7.4). Elution was done with a linear gradient of 25−500 mM NaCl in 20 mM tris, pH 7.4. Thioredoxin elutes between 100 and 125 mM NaCl. Following SDS−PAGE, purified fractions were pooled, concentrated by ultrafiltration with a 3 kDa cutoff membrane (Centriprep YM-3), and stored at −70 °C. The purity of the protein was analyzed on 15% SDS−PAGE. Wt*, 77c, 78c, and 79c proteins isolated were more than 95% pure, and the yields were ∼10 mg/L (except for 79c, which was ∼2 mg/L). In the case of 80c, although the protein showed a single band on SDS−PAGE, the overall yield of 0.1 mg/L was too low to accurately assess the purity. Protein concentrations were estimated using extinction coefficients calculated from the amino acid sequence (*21*). Values of extinction coefficients were 13 980 and 14 480 cm^{-1} M^{-1} for the oxidized state of Wt* and mutants (77c, 78c, 79c, and 80c), respectively. The value for Wt* is very similar to the value of 13 700 cm^{-1} M^{-1} reported previously (*22*) for wild-type thioredoxin.

Detection of Disulfide Bonds. Proteins in 6 M GdmCl were subjected to liquid chromatography coupled to electrospray ionization mass spectrometry (LC-MS). Masses for all the proteins were obtained in native as well as reducing conditions. Wt* showed a mass difference (mass reduced − mass oxidized) of 2 Da due to the presence of one disulfide bond in the wild-type protein, whereas the mutants showed a difference of 4 Da due to the presence of two disulfide bonds in each of the mutants. Formation of disulfide bonds was further confirmed by checking for the absence of free cysteines using a DTNB (5,5′-dithiobis-(2-nitrobenzoic acid)) assay as described previously (*23*).

Far-UV CD Spectroscopy and Fluorescence Spectroscopy. CD spectra were recorded on a Jasco J-715 C spectropolarimeter flushed with nitrogen gas. The spectra were recorded using a 0.1 cm path length cuvette with a scan rate of 10 nm/min and a time constant of 8 s. All data are an average over a minimum of six scans and are presented in terms of mean residue ellipticity (MRE) as a function of wavelength (*24*). Far-UV CD spectra were taken for all the proteins in the oxidized state at a concentration of approximately 4 μM in 10 mM phosphate, pH 7.0. Fluorescence measurements were carried out on solutions containing 2 μM Wt* or its mutants in CGH10, pH 7.0, without (for oxidized) and with (for reduced) 3 mM dithiothreitol in a thermostated 1 cm

path length cuvette in an Yvon-Horiba spectrofluorometer using an excitation wavelength of 280 nm.

Isothermal Melts of Protein with GdmCl at pH 7.0. The GdmCl denaturation curve for the oxidized proteins was determined by measuring the intrinsic fluorescence (280 nm excitation and 350 nm emission) of solutions containing 2 μM Wt* or its mutants as a function of GdmCl concentration. The fluorescence of thioredoxin in the oxidized state is strongly quenched by the active site disulfide (*25*). Consequently upon either reduction or denaturation, there is an increase in the intensity of tryptophan fluorescence. Ultrapure GdmCl was purchased from USB. GdmCl stock solutions were prepared, and their concentrations were determined by refractive index measurement. The intrinsic fluorescence readings were corrected for the fluorescence of GdmCl, which is 1−4% of the reading for Wt*. The solutions were incubated in 10 mM phosphate buffer, pH 7.0, at 25 °C for 6 or more hours to ensure that equilibrium was reached before the measurements were made. GdmCl-induced unfolding was completely reversible for all the proteins. The isothermal melts for the proteins under reduced condition were carried out by incubating the proteins with a 20-fold molar excess of DTT for 30 min prior to adding GdmCl. Since the fluorescence intensity difference between the unfolded protein and folded protein under reducing conditions was small, the isothermal denaturation experiments for the reduced proteins were monitored by CD at 222 nm as described previously (*26*).

Thermostability Measurement by Differential Scanning Calorimetry. DSC measurements in CGH10 buffer, pH 7.0, over the temperature range of 15−110 °C with a scan rate of 60 °C/h were performed using a VP-DSC microcalorimeter from Microcal, Inc. (Northampton, MA) as described previously (*27, 28*). The DSC data were analyzed with the ORIGIN software program (MicroCal) to determine the transition peak area and the temperature at which the excess heat capacity is maximum. For a two state transition, at this temperature (T_m), 50% of the molecules are unfolded.

Turbidimetric Assay of Insulin Reduction. All experiments were carried out at 298 K in a Jasco (V-530 UV/Vis) spectrophotometer. Each assay mixture contained 0.1 M phosphate buffer (pH 7.0), 2 mM EDTA, 0.13 mM porcine insulin, 0.33 mM dithiothreitol, and 7.8 μM thioredoxin. Following dithiothreitol addition, the absorbance of the mixture at 650 nm (A_{650}) was monitored as a function of time. The noncatalyzed reduction of insulin by dithiothreitol without thioredoxin and Wt* catalyzed insulin reduction were recorded as control experiments. The time taken for A_{650} to reach a value of 0.02 over a stable baseline was considered to be the time corresponding to the start of precipitation.

RESULTS

Characterization of Disulfides Spanning Adjacent Strands of a β Sheet. There were 58 disulfides found in the nonredundant database that bridged two adjacent strands of an antiparallel β sheet in a single protein chain (hereafter referred to as cross-strand disulfides). An additional four interchain cross-strand disulfides were also found. The number constitutes 3% of the total disulfides found in the same dataset. The dataset consisted of 17 097 pairs of antiparallel adjacent β strands out of which 7312 strands were

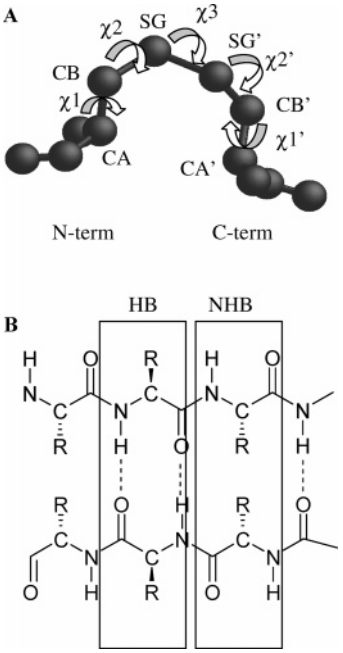

FIGURE 1: Schematic representations of various stereochemical parameters used to analyze cross-strand disulfide stereochemistry: (A) dihedral angle definitions; (B) two types of pairing possible between adjacent strands of antiparallel β sheet, hydrogen-bonded (HB) and non-hydrogen-bonded (NHB) pairs.

edge strands. The geometry of the disulfides was analyzed to see whether they were different from the disulfides found in other secondary structural elements. Geometrical parameters are described using the terminology discussed in Materials and Methods and summarized in Figure 1.

Comparison of Cross-Strand Disulfides and Other Disulfides in Terms of Torsion Angles and Strain. The distribution of χ_1, χ_2, χ_3, $\chi_{2'}$, and $\chi_{1'}$ for the cross-strand disulfides shows that the angles adopted by the cross-strand disulfides corroborate well with earlier studies on cross-strand disulfides (*12*) and small disulfide-rich folds (seven examples of cross-strand disulfides) (*29*). The mean angles for χ_1, χ_2, χ_3, $\chi_{2'}$, and $\chi_{1'}$ are centered about −50°, −85°, 105°, −85°, and −58°, respectively. The distribution of χ_3 is striking in terms of its preference for the right-handed rotamer. An earlier report has reported a similarly high prevalence of the right-handed rotamer at cross-strand disulfides in the case of small disulfide-rich proteins, where it has been defined as the right-handed staple conformation (*29*). The torsion energy of disulfides was calculated according to the torsion energy expression for disulfides defined in the leapf99 module of the AMBER program suite (*17*). This parameter has earlier been shown to correlate quite well with the stability of disulfides measured in vitro (*3*, *30*). The distributions of torsion energy for cross-strand disulfides and other disulfides are shown in Figure 2. The energy distribution shows that the cross-strand disulfides do not have significantly higher strain energy than other disulfides. This is in contrast to a recent report (*10*), which suggested that cross-strand disulfides are associated with higher torsional strain energy. The cross-strand disulfides have a preference to cross-link an edge strand with an adjacent inner strand. Only 13 out of 59 examples lacked an edge strand cysteine. The edge strands are accessible and hence might tolerate the distortion in the structure caused by the formation of disulfide by backbone

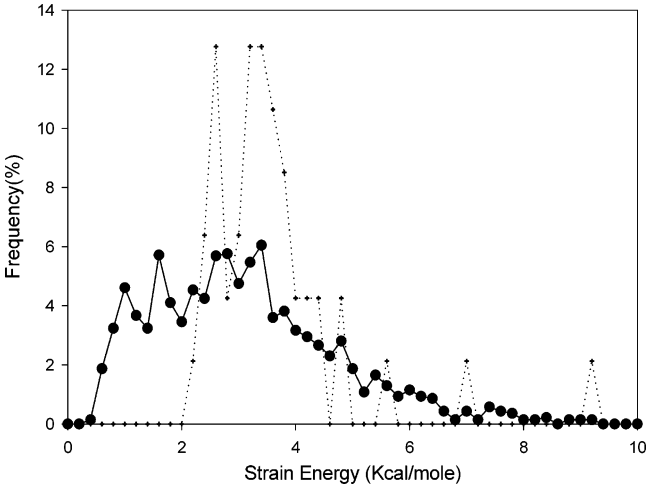

FIGURE 2: The frequency distribution of torsion strain energies of disulfides calculated from the AMBER force field using eq 1. The solid line shows the distribution for non-cross-strand disulfides, whereas the dashed line shows the distribution for cross-strand disulfides. The distribution shows that cross-strand disulfides are not significantly destabilized over other disulfides.

rearrangement without inducing significant strain in the protein structure.

Sequence Separation between Cysteine Pairs in Cross-Strand Disulfides. Disulfide stabilization of proteins is thought to result from a reduction in conformational entropy and consequent destabilization of the denatured state upon disulfide formation (*1*). The magnitude of the reduction in the conformational entropy of the denatured state will be a function of the sequence separation of the two cysteine residues as given by (*8*)

$$\Delta S = (-2.1 - 2.98 \ln N) \text{ cal mol}^{-1} \text{ K}^{-1} \qquad (2)$$

where ΔS is the stabilizing entropic effect and N is the loop length enclosed by the disulfide. Hence, we computed the frequency distribution of the sequence separation between half-cystines involved in cross-strand disulfides and compared it to the distribution of sequence separation between half-cystines in other disulfides (Figure 3A). The distribution indicates that the cross-strand disulfides cross-link residues that are, on average, closer in sequence compared to other disulfides. The average sequence separation between the middle residues of any two antiparallel strands of a β sheet was calculated. The distribution shows that the sequence separation between such residues in an edge strand and its adjacent strand is significantly lower than that between other adjacent strands. Only non-disulfide-bonded adjacent strands were considered to uncover any effect of disulfide on sequence separation. The distribution of sequence separation of cross-strand disulfides closely resembles the distribution for sequence separation involving edge strands and their adjacent strand. This indicated that the low sequence separation of cross-strand disulfides was induced by its presence on edge strands. The sequence separation between the middle residues of internal adjacent β strands did not have any marked preference for low sequence separation.

Distribution of φ and ψ for Cystines Involved in Cross-Strand Disulfides. To examine whether the distribution of φ and ψ for the cross-strand disulfides deviates significantly from the values adopted by non-cystine residues in antiparallel β strands, the average φ and ψ values were calculated for the two different populations. The mean φ and ψ for the cystines was $-122° \pm 14°$ and $142° \pm 34°$, and for non-cystine residues was $-112° \pm 26°$ and $130° \pm 43°$. When compared to the distribution for the angles adopted by non-cystine residues, it can be seen that the mean cystine geometry slightly deviates from the mean geometry of non-cystine residues but is well within the distribution allowed for non-cystine residues.

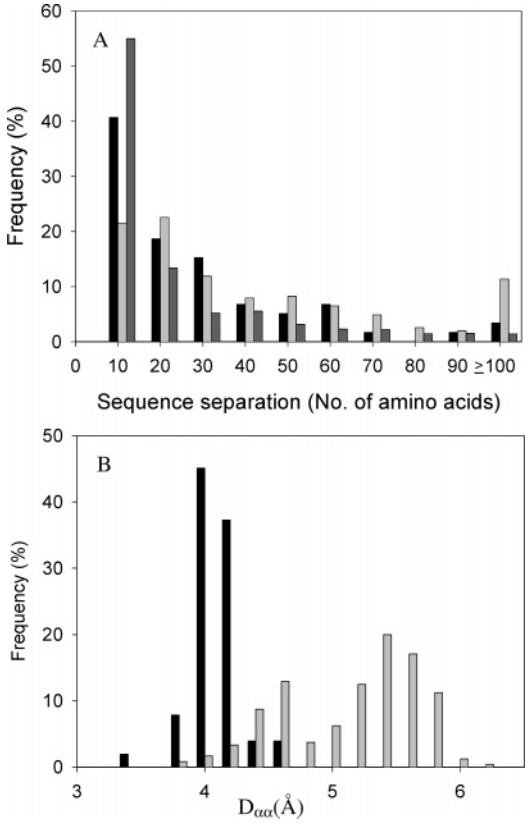

FIGURE 3: (A) Frequency distribution for sequence separation of three categories of residues. The sequence separation between the half-cystines of cross-strand disulfides (black bar) is significantly biased toward smaller sequence separation than that for non-cross-strand disulfides (light gray bar). The sequence separation between the middle residues of adjacent antiparallel β strands, one of which is an edge strand (dark gray bar), also shows a similar bias for smaller sequence separations. Since one of the half-cystines involved in cross-strand disulfides is generally found on an edge strand, the bias for smaller loop length of this type of disulfide is an imposed property. (B) The distribution of $C_\alpha - C_\alpha$ distance ($D_{\alpha\alpha}$) for non-cystine registered residues in antiparallel β-strands (grey bar) shows a bimodal distribution. The peak at 5.5 Å corresponds to hydrogen-bonded pairs, and the peak centered around 4.6 Å corresponds to non-hydrogen-bonded pairs. The distribution for cystines involved in cross-strand disulfides (black bar) is centered around 4 Å. The mean values of $D_{\alpha\alpha}$ for the non-cystine pairs are 4.4 ± 0.4 and 5.6 ± 0.4 Å for NHB and HB pairs, respectively. The mean for cross-strand disulfide is 4.0 ± 0.2 Å.

Distance Parameters. The normalized frequency distribution of the $C_\alpha - C_\alpha$ distance ($D_{\alpha\alpha}$) is shown for cross-strand disulfide pairs and non-cystine registered pairs in antiparallel β sheets (Figure 3B). Non-cystine pairs show a bimodal distribution of $D_{\alpha\alpha}$, which is due to the presence of two types of pairs in an antiparallel β sheet, hydrogen-bonded (HB) and non-hydrogen-bonded (NHB) (Figure 1B). Cross-strand disulfides show a unimodal distribution with the maximum being shifted toward a lower $D_{\alpha\alpha}$ of about 4 Å. This was

consistent with the fact that cross-strand disulfides are found exclusively at the NHB pairs (see below), which can accommodate a lower $D_{\alpha\alpha}$ than the hydrogen-bonded pair. This lower distance was found not to cause any steric clashes between the two strands. Thus, there was no evidence to suggest that naturally occurring cross-strand disulfides are conformationally strained.

Position of the Disulfides with Respect to Strand Registry. The distribution of cross-strand disulfides was striking in terms of positional preference. It was found that these disulfides occur only between NHB pairs of the adjacent strands. The positional preference was very strong. Only a single example where a cross-strand disulfide (PDB code 1b56, between position 120 and 127) (*31*) spans residues that are hydrogen bonded to each other was found in our dataset. However, this disulfide has an unusual χ_3 value of 160°.

In an ideal β sheet, for HB pairs $D_{\alpha\alpha} < D_{\beta\beta}$, whereas for NHB pairs $D_{\alpha\alpha} > D_{\beta\beta}$. The rotamer preference for naturally occurring cross-strand disulfides (g^+ g^+ dg^+ g^+) indicates that $D_{\alpha\alpha}$ should be smaller than $D_{\beta\beta}$, which is most likely to occur in the wide pair hydrogen-bonded position in an ideal β sheet (*29*). It was therefore previously reported that the formation of cross-strand disulfides should be more favorable at HB rather than at NHB pairs (*29*). Database analysis revealed that due to the pleated nature of naturally occurring β sheets, $D_{\alpha\alpha} < D_{\beta\beta}$ for both HB and NHB pairs. This comparison shows that NHB pairs can accommodate disulfides without major structural rearrangements in their naturally occurring geometry.

There could be two reasons for the absence of cross-strand disulfides at hydrogen-bonded positions in the dataset. First, such disulfides might result in strained conformations and hence decrease the stability or lead to a misfolded state and, therefore, would be selected against in evolution. Second, it is possible that due to the geometry of the hydrogen-bonded pair, disulfide bond formation is so strained that disulfides are not formed even if two cysteines are present.

The first possibility is supported by the fact that the only occurrence of a cross-strand disulfide at a HB pair, in 1b56, takes an unusual geometry in terms of the side chain torsion angle. The mean χ_3 for right-handed rotamers is centered at $+95° \pm 14°$, whereas the χ_3 value for the disulfide at the HB pair is 140°, more than two standard deviations off from the mean of the distribution for right-handed rotamers. The torsional strain energy of this disulfide is calculated to be 7.3 kcal mol^{-1}, which is about 4.1 kcal/mol higher than the mean torsional strain energy of a cross-strand disulfide. The torsional energy estimates are based on calculations rather than direct experimental measurement and appear to be somewhat high. Nevertheless, they provide a useful qualitative measure of whether a specific disulfide is strained relative to typical naturally occurring disulfides.

Biophysical Characterization of Cross-Strand Disulfide Mutants of Wt. E. coli* thioredoxin (Wt*) was chosen as a model system to study the effects of introduction of cross-strand disulfides on protein stability. Thioredoxin has a high level of expression and stability and is well characterized in terms of stability, structure, and folding (*9*, *26*, *32*−*34*). The database analysis described above indicated that cross-strand disulfides can be formed between the NHB pairs of an antiparallel β sheet and that one residue of the pair is generally found on an edge strand. We therefore designed four sets of mutants that would each have two cysteines introduced at either NHB pairs or HB pairs of a β sheet. One cysteine from each pair was at an exposed edge strand. Table 1 summarizes the data for the residues chosen for mutation and their distinction in terms of hydrogen bonding.

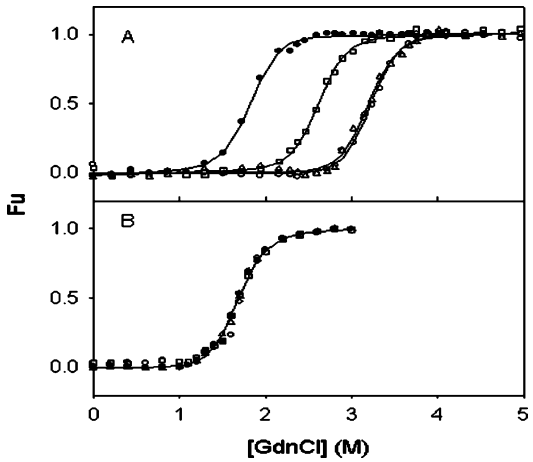

FIGURE 4: Isothermal chemical denaturation studies on Wt* and disulfide mutants of thioredoxin showing the fraction unfolded (fu) as a function of denaturant concentration for (A) oxidized and (B) reduced proteins at pH 7.0, 298 K. The symbols are 77c (○), 78c (●), 79c (△), and Wt* (□). In the oxidized state, 77c and 79c are stabilized, while 78c is destabilized relative to Wt*. In the reduced state, all proteins have similar stabilities. Data were fitted to a two-state model with globally fit *m* values of 3.7 and 3.6 kcal mol^{-1} M^{-1} for oxidized and reduced proteins, respectively. Unfolding of the oxidized and reduced proteins was monitored by fluorescence and CD spectroscopy, respectively.

Protein Expression, Purification, and Characterization of Disulfides. All the mutants are named according to the convention described in Materials and Methods. Mutants 77c and 79c were purified, and the yield was ∼10 mg/L of culture. The mutant 78c showed a moderate level of expression and could be purified with a yield of ∼2 mg/L. The mutant 80c showed high levels of expression but was largely present in the inclusion bodies. A small amount (∼0.1 mg/L) could be purified from the soluble fraction. Attempts to purify the protein from inclusion bodies failed, because the protein was exceptionally prone to aggregation and precipitation upon refolding. The mutants were characterized for disulfide formation using DTNB and also LC-MS. All the mutants had formed disulfides at the desired positions. This refutes the proposition that cross-strand disulfide formation is not possible at hydrogen-bonded pairs. Expression of 80c in the insoluble fraction suggested that a cross-strand disulfide at a HB pair might destabilize the protein. The low yield of 80c rendered it unsuitable for further biophysical analysis.

Spectroscopic and Thermodynamic Characterization of Proteins. All further studies were done on the remaining three mutants. Far-UV CD and fluorescence spectra were recorded for all the mutants, and the spectra were found to be similar to the Wt* spectrum (Figure 1, Supporting Information). This indicated that the secondary and tertiary structures of the mutants were identical to those of Wt*. Reversible denaturation studies of both oxidized and reduced thioredoxin have been reported previously (*9*, *26*, *33*, *35*). Figure 4 shows the isothermal denaturation curves for the mutants that were fitted to obtain the various stability parameters summarized

Table 2: The Stability of Wt* and Its Mutants in Oxidized and Reduced Conditions as Measured by Isothermal Denaturation Studies at 25 °C, pH 7.4, and DSC Studies

protein	$\Delta G°$ (25 °C) (kcal/mol)[b]	C_m (M)	$\Delta\Delta G°$ (25 °C) (kcal/mol)[c]	T_m (°C)[d] (DSC)	ΔT_m (°C)[d,e]	$\Delta\Delta H°$ (89.8 °C) (kcal/mol)[d,g]	$\Delta\Delta S$ (89.8 °C) (cal mol^{-1} K^{-1})[d,g]	$\Delta\Delta G°$ (89.8 °C) (kcal/mol)[g]
Wt*	9.6 ± 0.3	2.60		89.8				
77c	11.7 ± 0.4	3.15	2.1 ± 0.5	96.8	7.0	−19.2	−58.7	2.1
78c	6.7 ± 0.4	1.85	−2.9 ± 0.5	81.6	−7.2	−1.9	2.2	−2.7
79c	11.8 ± 0.4	3.20	2.2 ± 0.5	99.6	9.8	−27.7	−84.0	2.7
Wt*-red[a]	6.2 ± 0.4	1.70	−3.4 ± 0.5	75.3	*f*			
77c-red[a]	6.4 ± 0.3	1.72	−3.2 ± 0.5	75.0	−0.3			
78c-red[a]	6.3 ± 0.4	1.71	−3.3 ± 0.5	75.5	0.2			
79c-red[a]	6.3 ± 0.4	1.70	−3.3 ± 0.5	75.7	0.4			

[a] Under reduced conditions, in the presence of a 20-fold molar excess of DTT. [b] All isothermal melts were fitted with the same *m* value of −3.7 kcal mol^{-1} M^{-1} for oxidized and −3.6 kcal mol^{-1} M^{-1} for reduced proteins. [c] $\Delta\Delta G° = \Delta G°$(mutant) − $\Delta G°$(Wt*). [d] The average errors in T_m and $\Delta H°$ were 0.5 °C and 5 kcal mol^{-1}, respectively. Average errors in ΔT_m and $\Delta\Delta H°$ were estimated to be 0.7 °C and 7 kcal mol^{-1}, respectively, using propagation of errors. [e] $\Delta T_m = T_m$(mutant) − T_m(Wt*). [f] ΔT_m under reducing conditions is calculated with reference to reduced Wt* [g] Calculated as described previously using a ΔC_p value of 1.6 kcal mol^{-1} K^{-1} (*28*).

in Table 2. Wt* has a single disulfide bond at the catalytic site between Cys32 and Cys35 in the oxidized state. All mutants contain this disulfide as well as one additional engineered disulfide in the oxidized state. In the reduced state, Wt* and all mutants do not contain any disulfide. Denaturation was reversible in all cases. The NHB disulfide mutants, 77c and 79c, show an increase in stability of about 2.5 kcal mol^{-1} over WT*. The C_m of the mutants also increases by about 0.6 M GdmCl at 298 K. The HB mutant, 78c, shows a marked decrease in stability of about 3 kcal mol^{-1} below the wild-type protein. The C_m of this protein also decreases by 0.6 M GdmCl. Taken together with the fact that the 80c mutant was expressed largely in the insoluble fraction, this indicated that cross-strand disulfides at hydrogen-bonded pairs destabilize the protein. To reconfirm this result, we performed DSC studies of the three mutants (Figure 5). The results are summarized in Table 2. The mutants 77c and 79c showed a marked increase of 7 and 9.8 °C in melting temperature (T_m), respectively, whereas the 78c mutant shows a marked decrease of 8.2 °C in T_m. Measured values of $\Delta H°(T_m)$ and $\Delta S(T_m)$ for each of the mutant were extrapolated to a common reference temperature. This temperature was chosen to be the T_m of Wt* (89.8 °C). The extrapolation was carried out using the previously measured ΔC_p value for wild-type thioredoxin of 1.6 kcal mol^{-1} K^{-1} (*28*) as described previously. As expected, the stabilization obtained at NHB positions is associated with a reduction in the entropy of unfolding. However, the magnitude of $\Delta\Delta S$ is larger than expected from eq 2. The $\Delta\Delta G°$ values at 89.8 °C were 2.1 and 2.7 kcal mol^{-1} for 77c and 79c and −2.7 kcal mol^{-1} for 78c. The similarity of these values with $\Delta\Delta G°$ values obtained from isothermal denaturation experiments at 25 °C indicate that disulfide bonds at the NHB pairs have the capability to increase the stability of a protein over a wide range of temperatures.

Thermodynamic characterization of stability was also carried out with the reduced proteins to examine whether introduction of cysteines at any of the positions was the cause of the increase or decrease in stability. Since Wt* has one disulfide bond, we compared the stability of the reduced mutant proteins with reduced Wt*. Isothermal chemical denaturation experiments showed that the reduced mutants have the same stability as that of reduced Wt*. The DSC studies also show that the T_m's of the reduced mutants were equal to that of reduced Wt*. This clearly demonstrates that

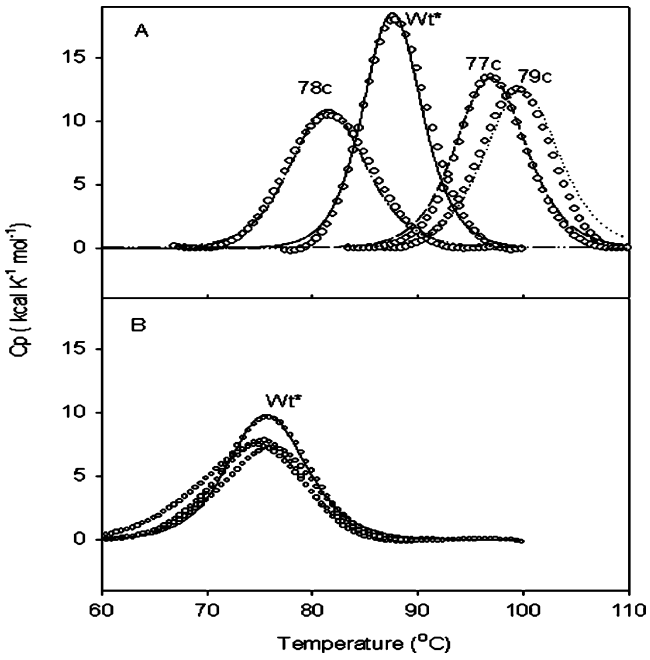

FIGURE 5: DSC studies on Wt* and disulfide mutants of thioredoxin at pH 7.0. (A) DSC scans of baseline subtracted excess heat capacity as a function of temperature for the oxidized proteins show that 78c is less stable than Wt*, whereas 77c and 79c are more stable than the Wt* protein. Raw data are shown as open circles, and the fitted data are shown as lines in all cases. (B) DSC scans for the reduced proteins show that all the proteins have similar thermal stability in the reduced state. The raw data (open circles) for the mutants are very similar and hence have not been labeled for clarity. The fitted data (black line) is shown only for Wt* for the sake of clarity.

the observed stability effects in the oxidized state are due to cross-strand disulfide formation. It should be noted that *E. coli* thioredoxin has exceptionally high thermal stability. Very few of the large number of mutants previously constructed have shown significantly enhanced thermal stability (*28*, *36*−*38*). The oxidized states of all the mutant proteins appear to have appreciably broader thermal transitions and a decreased cooperativity of unfolding relative to Wt*. This may be a consequence of increased order in the denatured states of these proteins as a consequence of disulfide formation. Similar decreases in cooperativity of thermal unfolding have been previously observed for engineered disulfide mutants of cellulase C, azurin, and avidin (*39*−*41*). In a counter

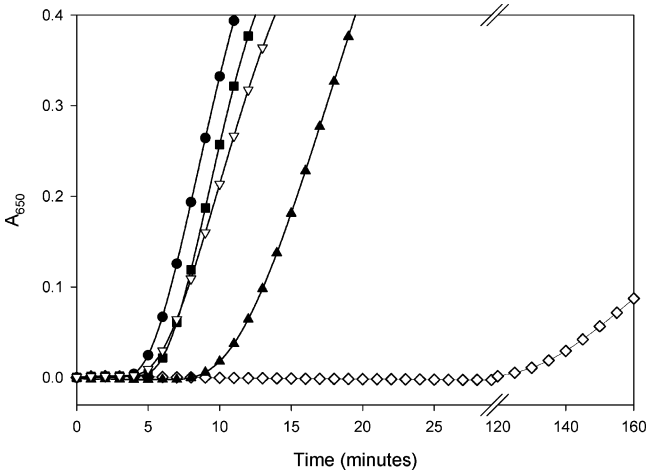

FIGURE 6: Thioredoxin-catalyzed reduction of insulin. Insulin aggregation following reduction was monitored by the increase in light scattering at 650 nm. Assay conditions were 0.1 M phosphate buffer, 2 mM EDTA, 0.13 mM procine insulin, 0.33 mM dithiothreitol, and 7.8 μM thioredoxin mutant. The symbols are (■) 77c, (▲) 78c, (●) 79c, and (▽) Wt*. Incubation mixture without thioredoxin (◊) served as control.

example, no decrease in cooperativity was seen in a disulfide engineered mutant of xylanase (*42*). For the reduced state of the thioredoxin mutants, there is only a slight decrease in cooperativity of unfolding. While Wt*, 77c, and 79c fit well to a two-state model, for 78c, the fit is poorer.

Thioredoxin-Catalyzed Insulin Reduction. The redox potential of the thioredoxin active site is thermodynamically linked to the difference in the free energy of the folding of the oxidized and reduced states of the protein (*43*). Hence, modulation of thioredoxin stability will affect the redox potential of the protein and can potentially affect its activity. We have therefore studied the ability of the thioredoxin derivatives to catalyze reduction of insulin by DTT. Reduction of insulin by dithiothreitol leads to cleavage of two interchain disulfides. Reduction is accompanied by formation of a white precipitate owing to insolubility of the insulin B chain. Thus, by quantitating the turbidity spectrophotometrically, one can monitor the rate of insulin reduction. Thioredoxin-catalyzed dithiothreitol reduction of insulin disulfides is a well characterized assay for determining thioredoxin activity (*44*). Insulin reduction was studied at pH 7.0 in an assay mixture containing final concentrations of 0.13 mM insulin and 0.33 mM dithiothreitol. In the control sample, containing only dithiothreitol, no precipitation was observed until 135 min. Addition of any one of Wt*, 77c, 78c, or 79c to a final concentration of 7.8 μM in the assay mixture resulted in rapid precipitation appearing after 5−10 min (Figure 6) as was previously reported for thioredoxin (*44*). In the case of 78c, the appearance of precipitate was slightly delayed when compared to the other mutants. However, all three thioredoxin disulfide mutants have a catalytic effect comparable to that of Wt* indicating that the changes in the thermodynamic stability have not greatly perturbed the activity, as measured by the above assay.

DISCUSSION

We have investigated whether disulfide bonds that bridge adjacent strands of antiparallel β sheets are unstable and whether they impart instability to protein structure. Previous

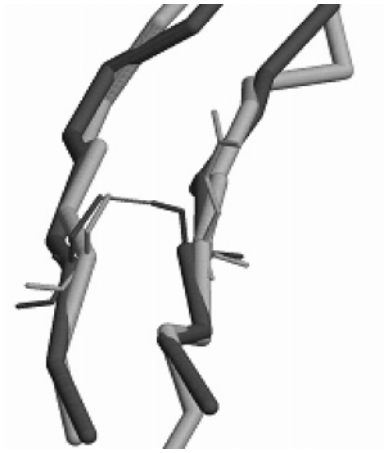

FIGURE 7: Structural superposition of two homologous proteins showing the change in geometry of the β sheet upon disulfide formation. Both proteins are in the SCOP family b.1.2.1. The protein 1axi (chain B) (dark gray) has a disulfide bond, whereas the analogous positions in 1eer (chain B) (light gray) do not. There is a small inward twist of one strand upon disulfide formation. There are also small changes in the backbone dihedral angles with the ϕ and ψ changing by an average of 10° and 27° at the $i-1$ positions, by 22° and 10° at ith positions, and by 7° and 20° at the $i+1$ positions.

studies had reported that cross-strand disulfides are unstable and can act as a molecular switch for conformational change of proteins (*10*). However, the present analysis of cross-strand disulfides provides the following insights. Although cross-strand disulfides are not very common, a number of such disulfides are present in the protein database. The conformational energy as judged by the distribution of side chain torsion angles and the torsion energy does not give any indication of this type of disulfide being strained. As judged from the distribution of φ and ψ, the β sheet is not significantly deformed at cross-strand cysteine pairs. In terms of their positional preference, these disulfides are only found at NHB pairs, and in most cases, one of the half cystines is present on an edge strand. The NHB pair geometry is distorted by a small inward twist due to the formation of the disulfide. This can be seen from the structural alignment of two homologous proteins belonging to the SCOP (*45*) family b.1.2.1.1 (Figure 7). One of the proteins has a cross-strand disulfide, and the other does not.

Cross-strand disulfides also show a marked decrease in sequence separation compared to the other disulfides. A similar low sequence separation was seen between the middle residues of an edge strand and its adjacent strand. Since most cross-strand disulfides involve an edge strand, the low sequence separation is induced by the high probability of hairpin occurrences at an edge strand. It is well-known from studies on synthetic peptides (*46*−*49*) that soluble hairpin formation in aqueous solution is difficult to achieve. Many of these peptides take up hairpin structure in solvents such as methanol and trifluoroethanol (TFE) whereas they are unstructured in water. This is attributed to solvent invasion of the interstrand hydrogen bonds in exposed β hairpins. Hence, though the sequence separation of the cross-strand disulfides is small, they might stabilize a protein structure by aiding in the formation of an edge β-hairpin in a β sheet that is exposed to solvent. We have also observed four occurrences of interchain disulfides between adjacent antiparallel strands formed by two different protein chains. The

disulfides in these cases were also observed to be exclusively at the NHB pairs, indicating that preference of cross-strand disulfides to form at NHB positions can be successfully used to cross-link chains of interacting proteins that form an extended sheet structure. This statement is also supported by an earlier study on Arc-repressor (*7*). It was reported that there was an increase in T_m of the Arc-repressor homodimer by 40 °C upon introduction of an intermolecular disulfide between engineered cysteine residues at position 11 on each chain. This position, upon inspection by us, also turned out to be a NHB pair and the resulting disulfide cross-linked adjacent antiprallel strands. In that study, sites were selected using a program (*50*) that did not make use of the fact that the disulfide would be at a NHB position. The particular site was chosen primarily because it involved making a mutation at a single residue, rather than two residues as with other sites, and the original asparagine residue present at the 11th position was exposed and would allow side chain rearrangements upon disulfide formation.

There were six examples in the present dataset where a cross-strand disulfide was not formed in the protein structure though two free cysteines were present at the NHB paired positions. Closer investigation revealed that these proteins were devoid of disulfides at any position, though they had a significant number of free cysteines and were localized in the cytoplasm or nucleus of the cell. This suggested that there was no evolutionary driving force for cross-strand disulfide formation in these cases because of the reducing environment of the cytoplasm.

The occurrence of cross-strand disulfides specifically at the NHB positions indicates that disulfides at HB positions are unfavorable. One possibility is that disulfide formation at these positions is geometrically not possible. However, a single example of a cross-strand disulfide between HB pairs (PDB 1b56) indicated that disulfide bonding is possible at the HB pairs. The other possibility is that disulfides at HB positions induce strain in the protein structure and hence are very rare. To test these hypotheses, we had designed disulfides in Trx at both HB and NHB positions. The results show that disulfide formation is sterically possible at all four positions nullifying the possibility that HB pairs are unlikely to form due to geometric constrains. Isothermal chemical denaturation experiments and DSC studies show that disulfides at HB positions cause significant destabilization of Trx, whereas the disulfides at NHB positions significantly stabilized the protein. This suggests that disulfides at HB positions destabilize proteins and hence were selected against during evolution. The increase in stability of 77c and 79c corroborated well with the expected value of about 3.1 kcal mol^{-1}, calculated from the length of the loop enclosed using eq 2.

In the absence of any steric effects, we would expect a similar increase in stability of 78c because of the similar loop length involved between the disulfide-bonded residues. The observed destabilization must therefore result from torsional strain in the engineered disulfide. The predicted increase in stability for 77c and 79c was obtained from models that take into account the loss of entropy of the unfolded state. The sign of $\Delta\Delta H$ and $\Delta\Delta S$ values for the mutants (Table 2) indicates that there is indeed a decrease in the entropy associated with unfolding of 77c and 79c. This change is seen to be absent in the case of 78c mutant. Mutant 77c is stabilized by 2.6 kcal/mol and 79c by 2.3 kcal/mol relative to Wt* at 25 °C and by 2.1−2.7 kcal/mol at 89.8 °C. These increases in stability compare favorably with the stability increase seen in other engineered disulfides (*5*, *51*−*53*), and this suggests that the cross-strand disulfide bonds are formed with little strain. Since, these disulfides can provide significant stability to a structure, modulation of their redox state has the ability to modulate the structural integrity of a protein. Introduction of cross-strand disulfides at NHB pairs involving one edge strand thus appears to be a simple and straightforward method to increase protein stability. Further studies with a variety of proteins will be required to test the above assertion.

SUPPORTING INFORMATION AVAILABLE

A table containing a list of proteins that were found to have a cross-stand disulfide bond and a figure showing CD and fluorescence spectra of thioredoxin mutants. The material is available free of charge via the Internet at http://pubs.acs.org.

REFERENCES

1. Harrison, P. M., and Sternberg, M. J. (1994) Analysis and classification of disulphide connectivity in proteins. The entropic effect of cross-linkage. *J. Mol. Biol. 244*, 448−463.
2. Creighton, T. E. (1988) Disulphide bonds and protein stability. *Bioessays 8*, 57−63.
3. Wells, J. A., and Powers, D. B. (1986) In vivo formation and stability of engineered disulfide bonds in subtilisin. *J. Biol. Chem. 261*, 6564−6570.
4. Guzzi, R., Andolfi, L., Cannistraro, S., Verbeet, M. P., Canters, G. W., and Sportelli, L. (2004) Thermal stability of wild type and disulfide bridge containing mutant of poplar plastocyanin. *Biophys. Chem. 112*, 35−43.
5. Clarke, J., Henrick, K., and Fersht, A. R. (1995) Disulfide mutants of barnase. I: Changes in stability and structure assessed by biophysical methods and X-ray crystallography. *J. Mol. Biol. 253*, 493−504.
6. Clarke, J., Hounslow, A. M., and Fersht, A. R. (1995) Disulfide mutants of barnase. II: Changes in structure and local stability identified by hydrogen exchange. *J. Mol. Biol. 253*, 505−513.
7. Robinson, C. R., and Sauer, R. T. (2000) Striking stabilization of Arc repressor by an engineered disulfide bond. *Biochemistry 39*, 12494−12502.
8. Pace, C. N., Grimsley, G. R., Thomson, J. A., and Barnett, B. J. (1988) Conformational stability and activity of ribonuclease T1 with zero, one, and two intact disulfide bonds. *J. Biol. Chem. 263*, 11820−11825.
9. Ladbury, J. E., Kishore, N., Hellinga, H. W., Wynn, R., and Sturtevant, J. M. (1994) Thermodynamic effects of reduction of the active-site disulfide of *Escherichia coli* thioredoxin explored by differential scanning calorimetry. *Biochemistry 33*, 3688−3692.
10. Hogg, P. J. (2003) Disulfide bonds as switches for protein function. *Trends. Biochem. Sci. 28*, 210−214.
11. Matthias, L. J., Yam, P. T., Jiang, X. M., and Hogg, P. J. (2003) Disulfide exchange in CD4. *Biofactors 17*, 241−248.
12. Richardson, J. S. (1981) The anatomy and taxonomy of protein structure. *Adv. Protein Chem. 34*, 167−339.
13. Wang, G., and Dunbrack, R. L., Jr. (2003) PISCES: a protein sequence culling server. *Bioinformatics 19*, 1589−1591.
14. Sayle, R. A., and Milner-White, E. J. (1995) RASMOL: biomolecular graphics for all. *Trends Biochem. Sci. 20*, 374.
15. Ho, B. K., and Curmi, P. M. (2002) Twist and shear in beta-sheets and beta-ribbons. *J. Mol. Biol. 317*, 291−308.
16. Dani, V. S., Ramakrishnan, C., and Varadarajan, R. (2003) MODIP revisited: reevaluation and refinement of an automated procedure for modeling of disulfide bonds in proteins. *Protein Eng. 16*, 187−193.
17. Weiner, S. J., Kollman, P. A., Case, D. A., Singh, U. C., Ghio, C., Alagona, G., Profeta, S., and Weiner, P. (1984) A New Force Field for Molecular Mechanical Simulation of Nucleic Acids and Proteins. *J. Am. Chem. Soc. 106*, 765−784.

18. Katti, S. K., LeMaster, D. M., and Eklund, H. (1990) Crystal structure of thioredoxin from *Escherichia coli* at 1.68 A resolution. *J. Mol. Biol. 212*, 167−184.
19. Sarkar, G., and Sommer, S. S. (1990) The "megaprimer" method of site-directed mutagenesis. *Biotechniques 8*, 404−407.
20. Ames, G. F., Prody, C., and Kustu, S. (1984) Simple, rapid, and quantitative release of periplasmic proteins by chloroform. *J. Bacteriol. 160*, 1181−1183.
21. Pace, C. N., Vajdos, F., Fee, L., Grimsley, G., and Gray, T. (1995) How to measure and predict the molar absorption coefficient of a protein. *Protein Sci. 4*, 2411−2423.
22. Holmgren, A., and Reichard, P. (1967) Thioredoxin 2: cleavage with cyanogen bromide. *Eur. J. Biochem. 2*, 187−196.
23. Ramachandran, S., and Udgaonkar, J. B. (1996) Stabilization of barstar by chemical modification of the buried cysteines. *Biochemistry 35*, 8776−8785.
24. Varadarajan, R., Sharma, D., Chakraborty, K., Patel, M., Citron, M., Sinha, P., Yadav, R., Rashid, U., Kennedy, S., Eckert, D., Geleziunas, R., Bramhill, D., Schleif, W., Liang, X., and Shiver, J. (2005) Characterization of gp120 and Its Single-Chain Derivatives, gp120-CD4D12 and gp120-M9: Implications for Targeting the CD4i Epitope in Human Immunodeficiency Virus Vaccine Design. *J. Virol. 79*, 1713−1723.
25. Holmgren, A. (1972) Tryptophan fluorescence study of conformational transitions of the oxidized and reduced form of thioredoxin. *J. Biol. Chem. 247*, 1992−1998.
26. Kelley, R. F., Shalongo, W., Jagannadham, M. V., and Stellwagen, E. (1987) Equilibrium and kinetic measurements of the conformational transition of reduced thioredoxin. *Biochemistry 26*, 1406−1411.
27. Prajapati, R. S., Lingaraju, G. M., Bacchawat, K., Surolia, A., and Varadarajan, R. (2003) Thermodynamic effects of replacements of Pro residues in helix interiors of maltose-binding protein. *Proteins 53*, 863−871.
28. Chakrabarti, A., Srivastava, S., Swaminathan, C. P., Surolia, A., and Varadarajan, R. (1999) Thermodynamics of replacing an alpha-helical Pro residue in the P40S mutant of *Escherichia coli* thioredoxin. *Protein Sci. 8*, 2455−2459.
29. Harrison, P. M., and Sternberg, M. J. (1996) The disulphide beta-cross: from cystine geometry and clustering to classification of small disulphide-rich protein folds. *J. Mol. Biol. 264*, 603−623.
30. Katz, B. A., and Kossiakoff, A. (1986) The crystallographically determined structures of atypical strained disulfides engineered into subtilisin. *J. Biol. Chem. 261*, 15480−15485.
31. Hohoff, C., Borchers, T., Rustow, B., Spener, F., and van Tilbeurgh, H. (1999) Expression, purification, and crystal structure determination of recombinant human epidermal-type fatty acid binding protein. *Biochemistry 38*, 12229−12239.
32. Bhutani, N., and Udgaonkar, J. B. (2003) Folding subdomains of thioredoxin characterized by native-state hydrogen exchange. *Protein Sci. 12*, 1719−1731.
33. Kelley, R. F., Wilson, J., Bryant, C., and Stellwagen, E. (1986) Effects of guanidine hydrochloride on the refolding kinetics of denatured thioredoxin. *Biochemistry 25*, 728−732.
34. Langsetmo, K., Fuchs, J., and Woodward, C. (1989) *Escherichia coli* thioredoxin folds into two compact forms of different stability to urea denaturation. *Biochemistry 28*, 3211−3220.
35. Ladbury, J. E., Wynn, R., Hellinga, H. W., and Sturtevant, J. M. (1993) Stability of oxidized *Escherichia coli* thioredoxin and its dependence on protonation of the aspartic acid residue in the 26 position. *Biochemistry 32*, 7526−7530.
36. Pedone, E., Saviano, M., Rossi, M., and Bartolucci, S. (2001) A single point mutation (Glu85Arg) increases the stability of the thioredoxin from *Escherichia coli*. *Protein Eng. 14*, 255−260.
37. Perez-Jimenez, R., Godoy-Ruiz, R., Ibarra-Molero, B., and Sanchez-Ruiz, J. M. (2005) The effect of charge-introduction mutations on *E. coli* thioredoxin stability. *Biophys. Chem. 115*, 105−107.
38. Gleason, F. K. (1992) Mutation of conserved residues in *Escherichia coli* thioredoxin: effects on stability and function. *Protein Sci. 1*, 609−616.
39. Nemeth, A., Kamondi, S., Szilagyi, A., Magyar, C., Kovari, Z., and Zavodszky, P. (2002) Increasing the thermal stability of cellulase C using rules learned from thermophilic proteins: a pilot study. *Biophys. Chem. 96*, 229−241.
40. Tigerstrom, A., Schwarz, F., Karlsson, G., Okvist, M., Alvarez-Rua, C., Maeder, D., Robb, F. T., and Sjolin, L. (2004) Effects of a novel disulfide bond and engineered electrostatic interactions on the thermostability of azurin. *Biochemistry 43*, 12563−12574.
41. Nordlund, H. R., Laitinen, O. H., Uotila, S. T., Nyholm, T., Hytonen, V. P., Slotte, J. P., and Kulomaa, M. S. (2003) Enhancing the thermal stability of avidin. Introduction of disulfide bridges between subunit interfaces. *J. Biol. Chem. 278*, 2479−2483.
42. Davoodi, J., Wakarchuk, W. W., Surewicz, W. K., and Carey, P. R. (1998) Scan-rate dependence in protein calorimetry: the reversible transitions of *Bacillus circulans* xylanase and a disulfide-bridge mutant. *Protein Sci. 7*, 1538−1544.
43. Lin, T. Y., and Kim, P. S. (1989) Urea dependence of thiol-disulfide equilibria in thioredoxin: confirmation of the linkage relationship and a sensitive assay for structure. *Biochemistry 28*, 5282−5287.
44. Holmgren, A. (1979) Thioredoxin catalyzes the reduction of insulin disulfides by dithiothreitol and dihydrolipoamide. *J. Biol. Chem. 254*, 9627−9632.
45. Murzin, A. G., Brenner, S. E., Hubbard, T., and Chothia, C. (1995) SCOP: a structural classification of proteins database for the investigation of sequences and structures. *J. Mol. Biol. 247*, 536−540.
46. Karle, I. L., Awasthi, S. K., and Balaram, P. (1996) A designed beta-hairpin peptide in crystals. *Proc. Natl. Acad. Sci. U.S.A. 93*, 8189−8193.
47. Regan, L. (1994) Protein structure. Born to be beta. *Curr. Biol. 4*, 656−658.
48. Das, C., Nayak, V., Raghothama, S., and Balaram, P. (2000) Synthetic protein design: construction of a four-stranded beta-sheet structure and evaluation of its integrity in methanol−water systems. *J. Pept. Res. 56*, 307−317.
49. Espinosa, J. F., Syud, F. A., and Gellman, S. H. (2002) Analysis of the factors that stabilize a designed two-stranded antiparallel beta-sheet. *Protein Sci. 11*, 1492−1505.
50. Pabo, C. O., and Suchanek, E. G. (1986) Computer-aided model-building strategies for protein design. *Biochemistry 25*, 5987−5991.
51. Matsumura, M., Signor, G., and Matthews, B. W. (1989) Substantial increase of protein stability by multiple disulphide bonds. *Nature 342*, 291−293.
52. Villafranca, J. E., Howell, E. E., Oatley, S. J., Xuong, N. H., and Kraut, J. (1987) An engineered disulfide bond in dihydrofolate reductase. *Biochemistry 26*, 2182−2189.
53. Kanaya, S., Katsuda, C., Kimura, S., Nakai, T., Kitakuni, E., Nakamura, H., Katayanagi, K., Morikawa, K., and Ikehara, M. (1991) Stabilization of *Escherichia coli* ribonuclease H by introduction of an artificial disulfide bond. *J. Biol. Chem. 266*, 6038−6044.

BI050921S